Prognostic Value of Multiparametric MRI-Based Radiomics model: Potential Role for Chemotherapeutic Benefits in Locally Advanced Rectal Cancer

Yanfen Cui
Shanxi Province Cancer Hospital
Wenhui Yang
Shanxi Bethune Hospital Cancer center
Jialiang Ren
GE Healthcare China
Dandan Li
Shanxi Province Cancer Hospital
Xiaosong Du
Shanxi Province Cancer Hospital
Junjie Zhang
Shanxi Province Cancer Hospital
Xiaotang Yang (yangxt210@126.com)
Shanxi Cancer Hospital

Research

Keywords: Radiomics, Magnetic Resonance Imaging, Locally advanced rectal cancer, Disease-free survival

Posted Date: July 27th, 2020

DOI: https://doi.org/10.21203/rs.3.rs-44982/v1

Version of Record: A version of this preprint was published at Radiotherapy and Oncology on January 1st, 2021. See the published version at https://doi.org/10.1016/j.radonc.2020.09.039.

Abstract

Background: Distant metastasis is the major cause of treatment failure in locally advanced rectal cancer (LARC). Adjuvant chemotherapy (AC) is usually used for distant control. However, only certain subgroups of patients could benefit from AC. Our aim was to develop a radiomics model for the prediction of survival and chemotherapeutic benefits using pretreatment multiparameter MR images and clinicopathological features in patients with LARC.

Methods: 186 consecutive patients with LARC underwent feature extraction from the whole tumor on T2-weighted (T2w), contrast enhanced T1-weighted (cT1w), and ADC images. Feature selection was based on feature stability and the Boruta algorithm. Radiomics signatures for predicting DFS (disease-free survival) were then generated using the selected features. Combining clinical risk factors, a radiomics nomogram was constructed using Cox proportional hazards regression model. The predictive performance was evaluated by Harrell's concordance indices (C-index) and time-independent receiver operating characteristic (ROC) analysis.

Results: Four features were selected to construct the radiomics signature, which was significantly associated with DFS ($P < 0.001$). The radiomics nomogram, incorporating radiomics signature and two clinicopathological variables (pN and tumor differentiation), exhibited better prediction performance for DFS than the clinicopathological model, with C-index of 0.780 (95%CI, 0.718-0.843) and 0.803 (95%CI, 0.717-0.889) in the training and validation cohorts, respectively. The radiomics nomogram-defined high-risk group had a shorter DFS, DMFS, and OS than those in the low-risk group (all $P <0.05$). Further analysis showed that patients with higher nomogram-defined score exhibited a favorable response to AC while the low-risk could not.

Conclusion: This study demonstrated that the newly developed pretreatment multiparameter MRI-based radiomics model could serve as a powerful predictor of prognosis, and may act as a potential indicator for guiding AC in patients with LARC.

Background

Outcome for patients with locally advanced rectal cancer (LARC) has improved over past decades, in part because of the use of neoadjuvant chemoradiotherapy (NCRT) followed by total mesorectal excision (TME) surgery (1, 2). The local recurrence (LR) rates has been dramatically reduced to less than 10%. However, these strategies may not necessarily improved survival, and distant metastasis (DM) is remain the major cause of treatment failure in LARC (3, 4). Additionally, adjuvant chemotherapy (AC) has been recommended for LARC to reduce the incidence of DM. However, it should be pointed out that only certain subgroups of patients could benefit from AC. Some studies have indicated AC is unnecessary in patients with pathological complete response (pCR) (5). Therefore, accurate prediction of the patient survival and guiding AC is of paramount importance to devise appropriate treatment and improve the prognosis of LARC.

Currently, risk assessment in survival of LARC is primarily based on the traditional TNM staging system (6–8). However, these clinicopathological risk factors provide inadequate prognostic information and do not evaluate the intrinsic biological heterogeneity of LARC. Moreover, it ignores the potentially pathological risk factors like tumor regression grade (TRG) and extramural venous invasion (EMVI) as well as more comprehensive information of the entire tumor that can be obtained from multiparameter MRI (4, 9, 10). Hence, the identification of new noninvasive prognostic biomarkers that allow assessment of tumor heterogeneity might be helpful for personalized medicine (11).

Nowadays, MRI has been widely in clinical workup to diagnose, stage, and monitor treatment response for rectal cancer, and can detect several prognostic factors (10, 12). Radiomics, converting these images into mineable high-dimensional features, has recently emerged as a promising method to evaluate tumor heterogeneity, as medical imaging can provide information regarding the underlying pathophysiology (13, 14). Thus, this strategy has been successfully used for tumor characterization, gene prediction, and therapy guidance in terms of rectal cancer (15–19). Few studies have evaluated the value of the heterogeneity of MR images, using texture or radiomics analyses, for predicting survival in LARC (20–22). However, they may suffer from small sample sizes, analysis of the single sequence or single section of tumor rather than whole-tumor volume analysis.

Therefore, the present study aims to determine the association between pretreatment multiparameter MRI-based radiomics signature and different survival in patients with LARC, and further establish a radiomics nomogram that incorporates the radiomics signature and clinicopathological findings for the individual prediction of survival.

Methods

Participant inclusion

Patients with rectal cancer treated at our hospital between December 2012 and November 2016 were reviewed and included for this study if they: (i) had locally advanced rectal adenocarcinoma (stage pre-CRT T2-weighted MR images as cT3/T4, and/or N-category positive) ; (ii) received pretreatment multiparameter MR images, including high-resolution T2WI, DWI, and contrast-enhanced T1-weighted MR imaging; (iii) treated by long-course NCRT followed by TME surgical resection. Flow chart of patient recruitment pathway was presented in Fig. 1. Institutional review board approval was acquired for this study, and written informed consent was waived owing to its retrospective nature.

Finally, 186 patients were enrolled and randomly divided into the training cohort (n = 131) and the validation cohort (n = 53) at a ratio of 7:3. Baseline characteristics, including age, gender, clinical T stage, N stage, histological grade, carcinoembryonic antigen (CEA), and carbohydrate antigen-199 (CA199), were obtained from medical records.

Neoadjuvant treatment and Surgery

All patients underwent three-dimensional conformal radiation therapy (gross tumor volume, 50–55 Gy; clinical target volume, 1.8–2.0 Gy; a total of 22 fractions). Concomitantly, capecitabine (800 mg/m^2 orally twice daily) was administered with radiation therapy. TME surgery was performed within 8 to 10 weeks (55 days on average, range 50–64 days) after the completion of NCRT. Afterward, patients received AC for 6 months, with the regimens of FOLFOX or XELOX. Reasons for not receiving AC included age, organ dysfunction suggestive of intolerance to treatment, and an individual patient's refusal.

Surgically resected specimens were evaluated by two dedicated pathologists, according to the Seventh American Joint Committee on Cancer (AJCC) TNM system (23). The tumor staging, lymph mode involvement, lymphovascular invasion (LVI), and lymphovascular invasion (PNI) were retrospectively collected. Additionally, the pathological TRG system was also evaluated according to the Mandard method (24).

Clinical endpoints and follow-up

Patients were followed up regularly after surgery, with 3-months intervals for the first 2 years, then 6-month intervals for the 3rd to 5th years, and annually thereafter. The main endpoint of this study was disease free survival (DFS), which was measured from the date of surgery until disease progression, death from any cause, or the last visit in follow up (censored), and nomograms were also built based on the DFS. Disease progression, including local recurrence and distant metastasis, were confirmed by clinical examination, imaging methods such as chest CT, and abdominopelvic CT or MRI, or biopsy-proven. Other endpoints included distant metastasis-free survival (DMFS, time from surgery to first distant metastasis) and overall survival (OS, time from surgery to death from any cause). The minimum follow-up period to confirm the 3-year DFS status was 36 months after the surgery, while the maximum follow-up period was 82 months (median, 44 months).

MRI protocol and Imaging segmentation

All patients underwent pretreatment multiparameter MRI. Detailed information on MRI protocol was presented in **Appendix E1.**

Oblique axial T2-weighted (T2W) and contrast enhanced T1-weighted (cT1W) images, as well as ADC images were retrieved from the picture archiving and communication system (PACS, Carestream, Canada) and then loaded into ITK-SNAP software (3.8.0, www.itksnap.org) for manual segmentation. A radiologist (reader 1) with 8 years of experience in pelvic MR imaging interpretation, outlined the whole-tumor volume of interests (VOIs), delineating along the border of the tumor and excluding the intestinal lumen on each slice. For ADC maps, VOIs were placed on the region of high signal intensity on DW images with b of 1000s/mm^2 first and then copied to the corresponding ADC maps, due to the higher resolution of DW images in comparison to ADC maps, while using all other image sequences as references.

Radiomics feature extraction

Before feature extraction, we standardized all above MR images by z-score normalization, and remove value out than 3 sigma in order to obtain a standard normal distribution of the image intensities. Afterward, all voxels were isotropically resampling into $1 \times 1 \times 1$ mm^3 using linear interpolation, and gray level of each image was quantized to 25 gray levels. Then a total of 1130 radiomics features quantifying phenotypic differences on the basis of first-order (n = 19), shape (n = 16), texture (n = 58), and wavelet and Laplacian of Gaussian (LoG) features, were exacted for each sequence by using PyRadiomics. More information about these features were presented in **Appendix E2**.

Feature Selection and Radiomics Signature building

We devised a two-step procedure for selecting robust features and reducing dimension. First, to calculate the inter-/intra-observer agreement of radiomics analysis, 30 patients were selected randomly and segmented again by reader 1 and another radiologist (reader 2) with 18 years of experience in a blind fashion one month later. The intra- and inter-class correlation coefficients (ICCs) were calculated, and radiomics features with both intra-observer and inter-observer ICCs values greater than 0.80 were selected for subsequent analysis. Second, the Boruta algorithm, a random forest-based wrapper method, was used to detect the key features for prediction (25). Boruta could select all relevant features instead of only the nonredundant ones. Then, the radiomics score (Radscore) was computed in the training cohort via multivariate cox regression model using the selected key features.

Development and validation of the radiomics nomogram

In the training cohort, the radiomics signature and all mentioned clinicopathological candidate predictors were tested in the univariate Cox proportional hazards model. Then, variables significant in the univariate analysis ($P < 0.05$) were considered for the multivariate Cox proportional hazard model to construct the radiomics nomogram for DFS prediction. To overcome the multicollinearity, backward stepwise selection with Akaike information criterion (AIC) was used as the stopping rule.

The potential association of the radiomics nomogram with DFS was first assessed in the training cohort and then tested in the validation cohort by using Kaplan-Meier survival analysis. The optimum cutoff value for classifying the patients into high-risk or low-risk groups according to the radiomics nomogram was identified by using the maximally selected rank statistics method. Stratified analyses were performed to explore the potential association of the radiomics nomogram with the DFS according to the clinicopathological risk factors from all patients. The prognostic performance of the model was evaluated by Harrell's concordance index (C-index) and time-dependent receiver operator characteristic (ROC) analysis.

To improve the stability of results, we repeated the randomized assignment and model building procedures four additional times. Subsequently, the mean C-index of the radiomics nomogram in the additional divisions was calculated.

Assessment of incremental value of radiomics signature in individual DFS estimation

To demonstrate the clinical benefits of the radiomics signature to the clinicopathological risk factors for individualized assessment of DFS in patient with LARC, we also developed a clinicopathological model, which incorporated only the independent clinicopathological risk factors. The calibration curves were generated to compare the predicted survival with the actual survival (26). The net reclassification improvement (NRI) were also quantified for evaluating the improvement of usefulness added by the radiomics signature (27). Finally, a decision curve analysis (DCA) was conducted to estimate the clinical usefulness of our radiomics nomogram by calculating of the net benefits at different threshold probabilities.

Statistical analysis

The differences regarding clinicopathological characteristics between the training and validation cohorts or between the high-risk and low-risk groups, were assessed by using an independent samples t test, Mann-Whitney U test, Chi-Squared tests, or Fisher exact test, where appropriate. Kaplan–Meier survival curves and the log-rank test were used to compare differences in the survival between the high-risk and low-risk groups. All statistical analyses were performed by using R software version 3.6.3 (http://www.R-project.org, **Appendix E3**). A two-sided P value of < 0.05 was considered statistically significant.

Results

Baseline information of participants

The patient characteristics were summarized in Table 1. The median follow-up time of the whole cohort was 44 months (range, 4–82 months). The training and validation cohorts were similar in terms of the clinicopathological characteristics (P = 0.373–0.906), except for the pre-CRT CEA level (P = 0.038). Regarding survival outcomes, 40 (30.5%) in the training cohort and 16 (29.1%) patients in the validation cohort experienced a confirmed disease progression (P = 0.845).

Table 1

Clinicopathological Characteristics of Patients with LARC in the Training cohort and Validation cohort			
Characteristics	**Training cohort n = 131**	**Validation cohort n = 55**	**P Value***
Age (years, mean ± SD)	54.15 ± 10.36	52.75 ± 11.38	0.415[a]
Gender (%)			0.700[b]
Male	77(58.8%)	34(61.8%)	
Female	54(41.2%)	21(38.2%)	
Tumor differentiation (%)			0.434[b]
well and moderate	111(84.7%)	49(89.1%)	
Poor	20(15.3%)	6(10.9%)	
Pre-CRT CEA (%)			0.038[b*]
≤ 5(Normal)	64(48.9%)	36(65.5%)	
> 5(Abnormal)	67(51.1%)	19(34.5%)	
Pre-CRT CA199 (%)			0.426[b]
≤ 20(Normal)	85(64.9%)	39(70.9%)	
> 20(Abnormal)	46(35.1%)	16(29.1%)	
Clinical stage (%)			0.932[b]
II	16(12.2%)	7(12.7%)	
III	115(87.8%)	48(87.3%)	
Clinical T stage (%)			0.545[b]
T3	87(66.4%)	41(74.5%)	
T4a	37(28.2%)	12(21.8%)	
T4b	7(5.3%)	2(3.6%)	
Clinical N stage (%)			0.717[b]
N0	12(9.2%)	7(12.7%)	
N1	73(55.7%)	28(50.9%)	
N2	46(35.1%)	20(36.4%)	

Clinicopathological Characteristics of Patients with LARC in the Training cohort and Validation cohort			
Pathological T stage (%)			0.906[c]
pT0	24(18.3%)	8(14.5%)	
pT1	4(3.1%)	1(1.8%)	
pT2	21(16.0%)	7(12.7%)	
pT3	28(21.4%)	13(23.6)	
pT4	54(41.2%)	26(47.3%)	
Pathological N stage (%)			0.751[c]
pN0	79 (60.3%)	28 (50.9%)	
pN1a	9 (6.9%)	6 (10.9%)	
pN1b	19 (14.5%)	9 (16.4%)	
pN1c	6 (4.6%)	2 (3.6%)	
pN2a	7(5.3%)	5 (9.1%)	
pN2b	11 (8.4%)	5 (9.1%)	
Pathological LVI (%)			0.373[b]
pLVI(-)	102 (77.9%)	46 (83.6%)	
pLVI(+)	29 (22.1%)	9 (16.4%)	
Pathological PNI (%)			0.861[b]
pPNI(-)	118 (88.5%)	50 (94.5%)	
pPNI(+)	13 (11.5%)	5 (5.5%)	
Mandard TRG			0.801[c]
1	24(18.3%)	7(12.7%)	
2	39(29.8%)	16(29.1%)	
3	38(29.0%)	17(30.9%)	
4	29(22.1%)	14(25.5%)	
5	1(0.8%)	1(1.8%)	
Adjuvant chemotherapy			0.372[b]
No	47 (35.9%)	16(29.1%)	

Clinicopathological Characteristics of Patients with LARC in the Training cohort and Validation cohort		
Yes	84 (64.1%)	39(70.9%)
Follow-up time (mo)		
Median†	43(29–43)	47(29–47)
Maximum	82	80
Abbreviations: CEA, carcinoembryonic antigen; LVI, lymphovascular invasion; PNI, perineural invasion.		
[a]student t test, [b]Pearson's Chi-squared test; [c]Fisher's Exact Test.		
†Data in parentheses are interquartile ranges. *P < 0.05.		

Radiomics Signature Construction and validation

Of 3930 extracted radiomic features for each patient, 2950 features (1048, 988, 914 features from T2W, ADC, and cT1W images, respectively) with high stability and reproducibility (both intra-observer and inter-observer ICCs > 0.80) were considered for subsequent analysis. Afterward, four key features were finally selected for the radiomics score building by the Boruta algorithm and stepwise select operation, with the calculation formula as following, Radscore=-0.5071 × ADC_wavelet.HHH_glrlm_HighGrayLevelRunEmphasis-0.2561 × cT1W_wavelet.LLH_glszm_ZoneEntropy + 0.5070 × cT1W_wavelet.HLL_glszm_SmallAreaLowGrayLevelEmphasis-0.6388 × T2w_original_glszm_SizeZoneNonUniformityNormalized. The distributions of the Radscore for each patient in the training and validation cohorts were shown in Fig. 2A and 2B. Similarly, the radiomics signature derived from each sequence were also constructed **(Appendix E4)**.

In the training cohort, the radiomics signature derived from joint the T2W, ADC, and cT1W images achieved better discriminatory ability for DFS prediction (C-index, 0.750; 95% confidence interval [CI]:0.669–0.831) than Radscore from either of them alone. Similarly, good prognostic performances were further confirmed in the validation cohort, with the corresponding C-index of 0.752 (95% CI, 0.638–0.866) **(**Table 2**).**

Table 2

Performance of models		
models	C-index(95%CI)	
	training cohort	validation cohort
Radiomics signature-T_2WI	0.582 (0.475–0.688)	0.659 (0.532–0.787)
Radiomics signature-ADC	0.627 (0.529–0.726)	0.658 (0.536–0.779)
Radiomics signature-cT_1WI	0.686 (0.599–0.774)	0.660 (0.540–0.802)
Radiomics signature-combined	0.750 (0.669–0.831)	0.752 (0.638–0.866)
Clinicopathological model	0.699 (0.627–0.771)	0.762 (0.650–0.873)
Radiomics nomogram	0.780 (0.718–0.843)	0.803 (0.717–0.889)
Abbreviations: HR, hazard ratio; CI, confidence interval.		

Table 3
Multivariate analysis of DFS in the training cohort

Characteristics	Hazard ratio (95% CI)	P Value
Tumor differentiation		
Well and moderate	Ref	
Poor	1.761(0.843-3.681)	0.033
Pathologic N stage		
pN0	Ref	
pN1a	2.626(0.738-9.341)	0.136
pN1b	3.440(1.479-8.000)	0.004
pN1c	3.772(0.795-17.893)	0.095
pN2a	7.106(2.286-22.088)	0.001
pN2b	3.454(1.335-8.941)	0.011
Radscore (low vs. high)	2.413(1.572-3.706)	5.69e-05

Development of an individualized prediction model

For the univariate analysis of DFS in the training cohort, a higher Radscore, higher CA199 level, poor differentiation, clinical T4a stage, ypT4 stage, pN1b and pN2 stage, pLVI, pPNI, and TRG4 were associated with worse DFS **(Table S1)**. In the multivariate Cox proportional hazard model, a higher

Radscore (HR, 2.413; 95% CI, 1.572–3.706; P < 0.001), pN1b stage (HR, 3.440; 95% CI, 1.479–8.000; P < 0.004), pN2a stage (HR, 7.106; 95% CI, 2.286–22.088; P < 0.001), pN2b stage (HR, 3.454; 95% CI, 1.335–8.941; P < 0.011), and poor differentiation (HR, 1.761; 95% CI, 0.843–3.681; P < 0.033) remained independent prognostic factors for DFS **(Table 3)**. Afterward, a radiomics nomogram that incorporated the above independent predictors for individualized DFS estimation was established and presented in Fig. 3A.

Performance and validation of the radiomics nomogram

For the training and validation cohorts, the C-indexes of the radiomics nomogram for DFS prediction were 0.780 (95% CI, 0.718–0.843) and 0.803 (95% CI, 0.717–0.889), respectively **(**Table 2**)**. The calibration curves of the radiomics nomogram for DFS at 1, 2, and 3 years were illustrated in Fig. 3B and 3C, which demonstrated better agreement between prediction and actual observation in both cohorts (both P□0.05). Moreover, the prognostic accuracy of the radiomics nomogram at 1, 2, and 3 years was also satisfactory **(**Fig. 4**).**

We identified the optimal radiomics nomogram-defined score for DFS prediction as 0.12. Accordingly, 71 (54.2%) and 27 (49.1%) patients with scores□0.12 were classified as the low-risk group for the training and validation cohorts, and 60 (45.8%) and 28 (50.9%) patients with scores ≥ 0.12 as high-risk group **(**Fig. 2C and 2D**)**.

The distribution of patients' clinicopathologic characteristics according to the dichotomized radiomics nomogram was presented in **Table S2**. Kaplan–Meier curves showed that higher radiomics nomogram-defined score were significantly associated with worse DFS, and the corresponding 3-year DFS rates were 46.7% and 91.4% for the high-risk versus low-risk group in the training cohort (HR, 7.76; 95% CI, 3.42–17.60; P < 0.0001), and 53.6% and 92.6% in the validation cohort (HR, 8.94; 95% CI, 2.03–39.42; P < 0.0005), respectively (Fig. 5A-B). Meanwhile, patients in the high-risk group also achieved worse DMFS and OS (all P < 0.05; Fig. 5C-F).

We further evaluated the prognostic value of radiomics nomogram on the basis of various clinicopathologic risk factors in the whole cohorts. The stratified analyses revealed that the radiomics nomogram remained a powerful and statistically significant prognostic predictor **(Figure S1)**. Moreover, the mean C-index of the additional four divisions was 0.772 (95% CI, 0.722–0.802) in radiomics nomogram.

Assessment of incremental value of radiomics signature in individual DFS estimation

When we removed the signature from the radiomics nomogram and kept only two statistically significant features (pN and tumor differentiation) for building the clinicopathological model, the C-index dropped to 0.699 (95% CI: 0.627–0.771) in the training cohort and 0.762 (95% CI: 0.650–0.873) in the validation cohort, respectively **(**Table 2**)**. The integration of MRI-based radiomics signature into the nomogram

yielded a total NRI 0.207 (95% CI: 0.045–0.353) for DFS, indicating improved classification accuracy for survival outcomes. Furthermore, the radiomics nomogram was identified as the best model, with the lowest AIC (344.8) value compared with the clinicopathological model (AIC = 539.7) or the radiomics signature (AIC = 447.6). Additionally, time-independent ROC analysis also validated that the radiomics nomogram had the best prognostic power **(Figure S2).**

The DCA showed that the radiomics nomogram was superior to the radiomics signature and the clinicopathological model over most of the range of reasonable threshold probabilities, indicating the incremental value of nomogram in terms of clinical application **(**Fig. 6**)**.

Benefit of adjuvant chemotherapy

For the whole cohort, survival outcomes were comparable between AC and no-AC groups **(**all P□0.05, **Figure S3)**. We then applied our radiomics nomogram to detect whether patients could benefit from AC. Within the high-risk group, patients receiving AC (n = 59) achieved significantly better 3-year DFS (59.3% vs. 27.6%, P = 0.0017), DMFS (64.1% vs. 34.5%, P = 0.0089), and OS (74.6% vs. 55.2%, P = 0.030) rates than those did not receive AC (n = 29) **(**Fig. 7**)**. However, for the 98 patients with low-risk, there was no significant difference in the 3-year DFS (90.5% vs. 94.1%, P = 0.418), DMFS (100.0% vs. 90.5%, P = 0.052), and OS (95.3% vs. 94.1%, P = 0.706) rates between patients who received AC (n = 64) and no-AC (n = 34) groups.

Discussion

In the current study, we not only investigate the prognostic value of pretreatment multiparametric MRI-based radiomics signature in patients with LARC, but also successfully develop and validate a radiomics nomogram, which was powerful in risk stratification and was able to predict DFS, DMFS and OS better than the current clinicopathological model. More importantly, the proposed radiomics nomogram might help identify which patients are expected to benefit from AC, indicating that it might be helpful for the future management of LARC.

Personalized medicine in cancer patients implies identifying imaging biomarkers to predict survival. To this end, texture analysis of different modalities has been used in LARC patients, with varying degrees of success. In a series of 56 patients with LARC, Jalil et al. identified the mean of positive pixels (MPP) of T2WI as an independent predictor of DFS and OS (20). Similarly, Lovinfosse et al. showed that the texture parameter coarseness of baseline 18F-FDG PET/CT was associated with disease-specific survival (DSS) and with DFS of LARC (28). Chee et al. also found a significant correlation between homogeneous texture features and higher DFS in 95 patients with LARC (29). All these prior studies have typically focused on few radiomics features, which seems intuitive and might underestimated the significance of radiomics. Therefore, construction of multifactor panels is a more common approach to overcome this challenge in outcome estimation.

Radiomics hypothesizes that the intratumor heterogeneity, which was difficult to detect visually, could be exhibited on the spatial distribution of voxel intensities. For the construction of radiomics signature, 3930 candidate features were reduced to only four predictors. Intriguingly, all selected features were GLSZM/GLRLM-related features, which could take into account the interaction between neighboring pixels and were well suited to measure different aspects of textural heterogeneity within the tumor (30). Moreover, wavelet features, which could reflect multi-frequency information at different scales unrecognized by the naked eye to quantify tumor heterogeneity, were the majority used in our optimal radiomics signature (3/4), similar to other MRI-based radiomics studies (16, 31).

As demonstrated in the present study, the identified radiomics signature from joint T2W, ADC, and cT1W images performed better than those from either of them alone, and was also an independent risk factor of DFS in the patients with LARC, with C-index of 0.750 and 0.752 in the training and validation cohort, respectively. A possible explanation is that the multi-sequences used in our study reflected different aspects of tumor, such as tumor intensity, cellularity, and vascularization, and a combination of them might reflect much more comprehensive information of the tumors and improve prognostication. Moreover, the performance of our radiomics signature was superior to those derived from CT or PET/CT images, with the C-index about 0.650 (32, 33). This has been confirmed by our study that the Radscore values were significant higher in the patients with progressive disease. That is, tumors with higher intratumoral heterogeneity, are more likely to be resistant to NCRT and have a poorer prognosis (18).

Furthermore, the radiomic nomogram, incorporating radiomics signature and clinicopathological factors, had significantly better ability to predict DFS than the clinicopathological model, with a higher C-index of 0.803 and positive NRI and lowest AIC, consistent with the results of Meng and Jeon et al (21, 22). The results of time-independent ROC analysis further support this conclusion. This may be because the clinicopathological features only reflect specific tumor information, while multiparametric MRI-based radiomics can comprehensively and quantifiably characterize the tumor phenotype, and thus provide a robust way to characterize the intratumoral heterogeneity noninvasively. Additionally, the radiomics nomogram's good ability to predict DMFS and OS, also confirmed its prognostic value, which could be used to stratify patients into corresponding high and low risks groups.

Currently, AC, given after TME, has been recommend for most LARC patients, and has proved to be a powerful a robust tool against DM. However, not all patients will benefit from chemotherapy efficacy. Given these, it would be of great importance to identify patients with AC benefit. Previous studies have developed valuable radiomics models derived from different modalities, to identify patients with various cancers who will benefit from different therapies (34–36). Our findings are consistent with above statement that high-risk patients could benefit from AC and more intensive observation and aggressive treatment regimens should be considered in these cases. These findings provided a novel tool for guiding AC.

Nevertheless, some notes should be emphasized. Firstly, pN and tumor differentiation were identified as independent prognostic factors for DFS in our study, partly consistent with previous studies (22, 28, 33).

Even so, a single considered strong risk factor, could hardly assess the comprehensive outcome of individual patients. In contrast, the nomogram, taking into account multiple risk factors, could provide more informative metrics and an easy-to-use tool for clinicians. Secondly, whole-tumor VOIs, rather than signal largest slice ROIs, could provide a robust way to characterize the heterogeneity of the entire lesion, and reduce concerns of selection bias. Lastly, although lacked external validation, the clinical utility of radiomic nomogram was assessed by DCA, confirming the incremental value of signature to clinicopathological model for individualized estimation.

Some limitations of our study should be acknowledged. The first is the limited sample size and the retrospective nature of data collection. Further prospective studies involving a larger population are needed to validate our model. Second, study data were collected from a single center. Although we have performed four additional divisions with good results, external validation should be warranted in the future. Third, the follow-up duration was not long enough, thus, we constructed the radiomics model primarily base on DFS. Finally, various modalities, pathological imaging, genomic sequencing, and molecular biomarkers, as well as some MRI morphologic characteristics, should be investigated and construct a more stable and accurate model, for tailored treatment into the era of personalized medicine.

Conclusions

In summary, we identified a multiparametric MRI-based radiomics signature as a powerful approach for predicting prognosis in patients with LARC, and improved the prognostic ability of the clinicopathological model. Additonally, the developed radiomics nomogram successfully classify patients into high- and low-risk groups for all endpoints, and thereby might provide a novel tool for guiding AC and individualized treatment strategies. Finally, future prospective multicenter studies with considerably large cohorts are needed to validate our findings.

Abbreviations

LARC: locally advanced rectal cancer; NCRT: neoadjuvant chemoradiotherapy; TME: total mesorectal excision; LR: local recurrence; DM: distant metastasis; AC: adjuvant chemotherapy; pCR: pathologic complete response; TRG: tumor response grading; EMVI: extramural venous invasion; CEA: carcinoembryonic antigen; CA199: carbohydrate antigen-199; LVI: lymphovascular invasion; PNI: perineural invasion; DFS: disease free survival; DMFS: distant metastasis-free survival; OS: overall survival; VOIs: volume of interests; LoG: Laplacian of Gaussian; ICC: interclass correlation coefficient; NRI: net reclassification improvement; DCA: decision curve analysis

Declarations

Ethics approval and consent to participate

Institutional review board approval was acquired for this study, and written informed consent was waived owing to its retrospective nature.

Consent for publication

Not applicable.

Availability of data and material

The datasets during and/or analysed during the current study available from the corresponding author on reasonable request.

Competing interests

The authors declare that they have no competing interests.

Funding

This study was supported by the Applied Basic Research Programs of Shanxi Province (No. 201801D121307 and 201801D221390) and the Youth Project of Shanxi Provincial Health Commission (No. 2019058). The funders had no role in study design, data collection and analysis, decision to publish, or preparation of the manuscript.

Author contributions

Conception and design: Yanfen Cui, Xiaotang Yang.

Data collection: Yanfen Cui, Wenhui Yang, Dandan Li, Xiaosong Du.

Data analysis: Yanfen Cui, Jialiang Ren, Junjie Zhang.

Manuscript writing: Yanfen Cui, Wenhui Yang.

Manuscript review: Xiaotang Yang.

Final approval of manuscript: All authors.

Acknowledgments

Not applicable.

References

1. Chen W, Zheng R, Baade PD, et al. Cancer statistics in China, 2015. Cancer J Clin. 2016;66(2):115–32.
2. Kapiteijn E, Marijnen CA, Nagtegaal ID, et al. Preoperative radiotherapy combined with total mesorectal excision for resectable rectal cancer. N Engl J Med. 2001;345(9):638–46.
3. van Gijn W, Marijnen CA, Nagtegaal ID, et al. Preoperative radiotherapy combined with total mesorectal excision for resectable rectal cancer: 12-year follow-up of the multicentre, randomised controlled TME trial. The Lancet Oncology. 2011;12(6):575–82.
4. Fokas E, Liersch T, Fietkau R, et al. Tumor regression grading after preoperative chemoradiotherapy for locally advanced rectal carcinoma revisited: updated results of the CAO/ARO/AIO-94 trial. Journal of clinical oncology: official journal of the American Society of Clinical Oncology. 2014;32(15):1554–62.
5. Maas M, Nelemans PJ, Valentini V, et al. Adjuvant chemotherapy in rectal cancer: defining subgroups who may benefit after neoadjuvant chemoradiation and resection: a pooled analysis of 3,313 patients. International journal of cancer. 2015;137(1):212–20.
6. Valentini V, van Stiphout RG, Lammering G, et al. Nomograms for predicting local recurrence, distant metastases, and overall survival for patients with locally advanced rectal cancer on the basis of European randomized clinical trials. Journal of clinical oncology: official journal of the American Society of Clinical Oncology. 2011;29(23):3163–72.
7. Sun Y, Lin H, Lu X, et al. A nomogram to predict distant metastasis after neoadjuvant chemoradiotherapy and radical surgery in patients with locally advanced rectal cancer. Journal of surgical oncology. 2017;115(4):462–9.
8. Merkel S, Weber K, Schellerer V, et al. Prognostic subdivision of ypT3 rectal tumours according to extension beyond the muscularis propria. Br J Surg. 2014;101(5):566–72.
9. Patel UB, Taylor F, Blomqvist L, et al. Magnetic resonance imaging-detected tumor response for locally advanced rectal cancer predicts survival outcomes: MERCURY experience. Journal of clinical oncology: official journal of the American Society of Clinical Oncology. 2011;29(28):3753–60.
10. Zhang XY, Wang S, Li XT, et al. MRI of Extramural Venous Invasion in Locally Advanced Rectal Cancer: Relationship to Tumor Recurrence and Overall Survival. Radiology. 2018;289(3):677–85.
11. O'Connor JP, Aboagye EO, Adams JE, et al. Imaging biomarker roadmap for cancer studies. Nature reviews Clinical oncology. 2017;14(3):169–86.
12. Taylor FG, Quirke P, Heald RJ, et al. Preoperative magnetic resonance imaging assessment of circumferential resection margin predicts disease-free survival and local recurrence: 5-year follow-up results of the MERCURY study. Journal of clinical oncology: official journal of the American Society of Clinical Oncology. 2014;32(1):34–43.
13. Aerts HJ, Velazquez ER, Leijenaar RT, et al. Decoding tumour phenotype by noninvasive imaging using a quantitative radiomics approach. Nature communications. 2014;5:4006.

14. Lambin P, Leijenaar RTH, Deist TM, et al. Radiomics: the bridge between medical imaging and personalized medicine. Nature reviews Clinical oncology. 2017;14(12):749–62.
15. Cui Y, Liu H, Ren J, et al. Development and validation of a MRI-based radiomics signature for prediction of KRAS mutation in rectal cancer. European radiology. 2020;30(4):1948–58.
16. Liu Z, Zhang XY, Shi YJ, et al. Radiomics Analysis for Evaluation of Pathological Complete Response to Neoadjuvant Chemoradiotherapy in Locally Advanced Rectal Cancer. Clinical cancer research: an official journal of the American Association for Cancer Research. 2017;23(23):7253–62.
17. Liu H, Zhang C, Wang L, et al. MRI radiomics analysis for predicting preoperative synchronous distant metastasis in patients with rectal cancer. European radiology. 2019;29(8):4418–26.
18. Cui Y, Yang X, Shi Z, et al. Radiomics analysis of multiparametric MRI for prediction of pathological complete response to neoadjuvant chemoradiotherapy in locally advanced rectal cancer. European radiology. 2019;29(3):1211–20.
19. Horvat N, Veeraraghavan H, Khan M, et al. MR Imaging of Rectal Cancer: Radiomics Analysis to Assess Treatment Response after Neoadjuvant Therapy. Radiology. 2018;287(3):833–43.
20. Jalil O, Afaq A, Ganeshan B, et al. Magnetic resonance based texture parameters as potential imaging biomarkers for predicting long-term survival in locally advanced rectal cancer treated by chemoradiotherapy. Colorectal disease: the official journal of the Association of Coloproctology of Great Britain Ireland. 2017;19(4):349–62.
21. Jeon SH, Song C, Chie EK, et al. Delta-radiomics signature predicts treatment outcomes after preoperative chemoradiotherapy and surgery in rectal cancer. Radiation oncology. 2019;14(1):43.
22. Meng Y, Zhang Y, Dong D, et al. Novel radiomic signature as a prognostic biomarker for locally advanced rectal cancer. Journal of magnetic resonance imaging: JMRI. 2018.
23. Edge SB, Compton CC. The American Joint Committee on Cancer: the 7th edition of the AJCC cancer staging manual and the future of TNM. Ann Surg Oncol. 2010;17(6):1471–4.
24. Mandard AM, Dalibard F, Mandard JC, et al. Pathologic assessment of tumor regression after preoperative chemoradiotherapy of esophageal carcinoma. Clinicopathologic correlations. Cancer. 1994;73(11):2680–6.
25. Kursa MB, Rudnicki WR. Feature Selection with the Boruta Package. J Stat Softw. 2010;36(11):1–13.
26. Kramer AA, Zimmerman JE. Assessing the calibration of mortality benchmarks in critical care: The Hosmer-Lemeshow test revisited. Critical care medicine. 2007;35(9):2052–6.
27. Pencina MJ, D'Agostino RB, Sr., Steyerberg EW. Extensions of net reclassification improvement calculations to measure usefulness of new biomarkers. Statistics in medicine. 2011;30(1):11–21.
28. Lovinfosse P, Polus M, Van Daele D, et al. FDG PET/CT radiomics for predicting the outcome of locally advanced rectal cancer. Eur J Nucl Med Mol Imaging. 2018;45(3):365–75.
29. Chee CG, Kim YH, Lee KH, et al. CT texture analysis in patients with locally advanced rectal cancer treated with neoadjuvant chemoradiotherapy: A potential imaging biomarker for treatment response and prognosis. PloS one. 2017;12(8):e0182883.

30. Davnall F, Yip CS, Ljungqvist G, et al. Assessment of tumor heterogeneity: an emerging imaging tool for clinical practice? Insights into imaging. 2012;3(6):573–89.
31. Zhou X, Yi Y, Liu Z, et al. Radiomics-Based Pretherapeutic Prediction of Non-response to Neoadjuvant Therapy in Locally Advanced Rectal Cancer. Ann Surg Oncol. 2019;26(6):1676–84.
32. Li H, Boimel P, Janopaul-Naylor J, et al. Deep Convolutional Neural Networks for Imaging Data Based Survival Analysis Of Rectal Cancer. Proceedings IEEE International Symposium on Biomedical Imaging. 2019;2019:846-9.
33. Wang J, Shen L, Zhong H, et al. Radiomics features on radiotherapy treatment planning CT can predict patient survival in locally advanced rectal cancer patients. Scientific reports. 2019;9(1):15346.
34. Jiang Y, Chen C, Xie J, et al. Radiomics signature of computed tomography imaging for prediction of survival and chemotherapeutic benefits in gastric cancer. EBioMedicine. 2018;36:171–82.
35. Peng H, Dong D, Fang MJ, et al. Prognostic Value of Deep Learning PET/CT-Based Radiomics: Potential Role for Future Individual Induction Chemotherapy in Advanced Nasopharyngeal Carcinoma. Clinical cancer research: an official journal of the American Association for Cancer Research. 2019;25(14):4271–9.
36. Zhang LL, Huang MY, Li Y, et al. Pretreatment MRI radiomics analysis allows for reliable prediction of local recurrence in non-metastatic T4 nasopharyngeal carcinoma. EBioMedicine. 2019;42:270–80.

Figures

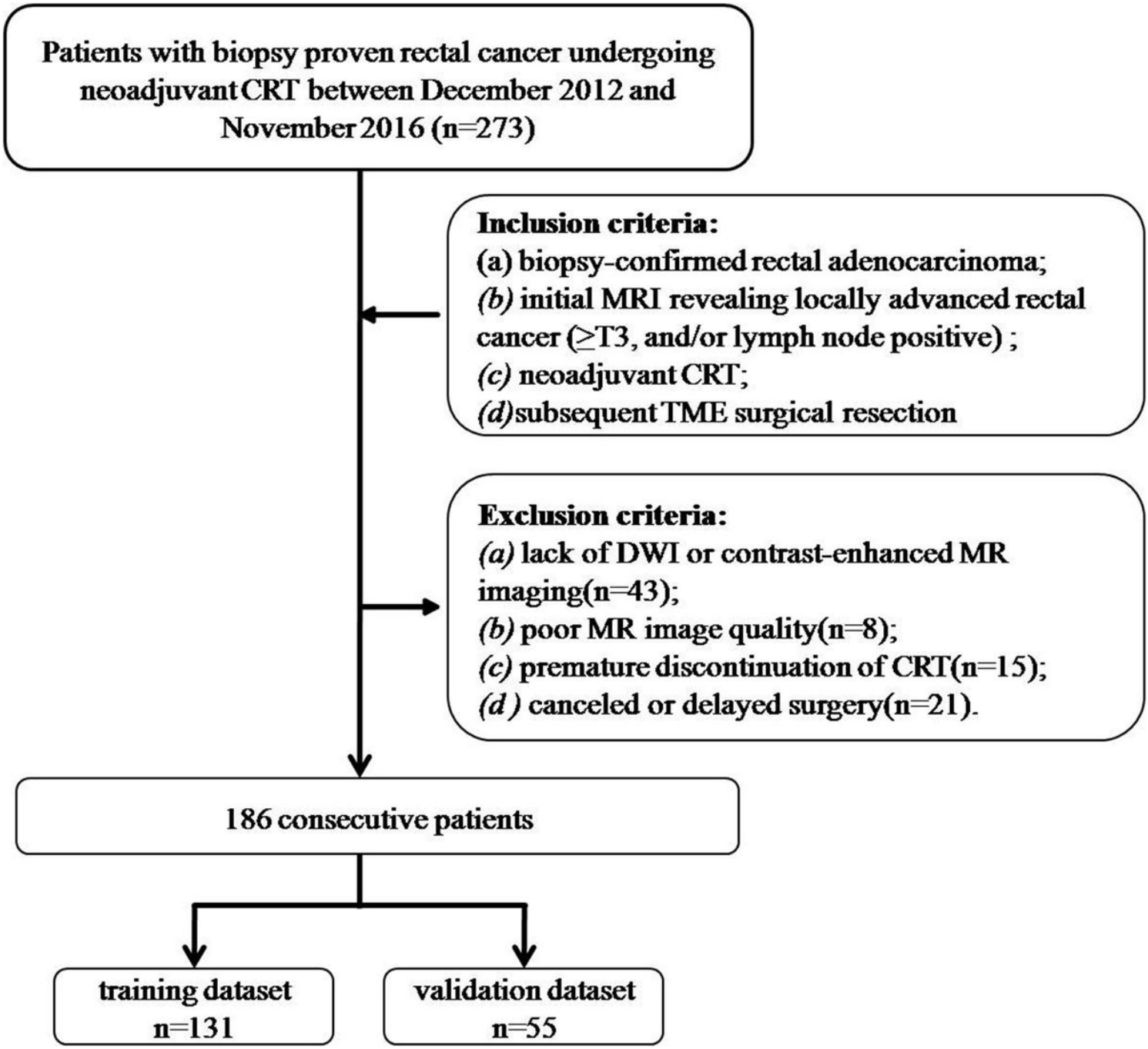

Figure 1

Recruitment pathway for patients in this study.

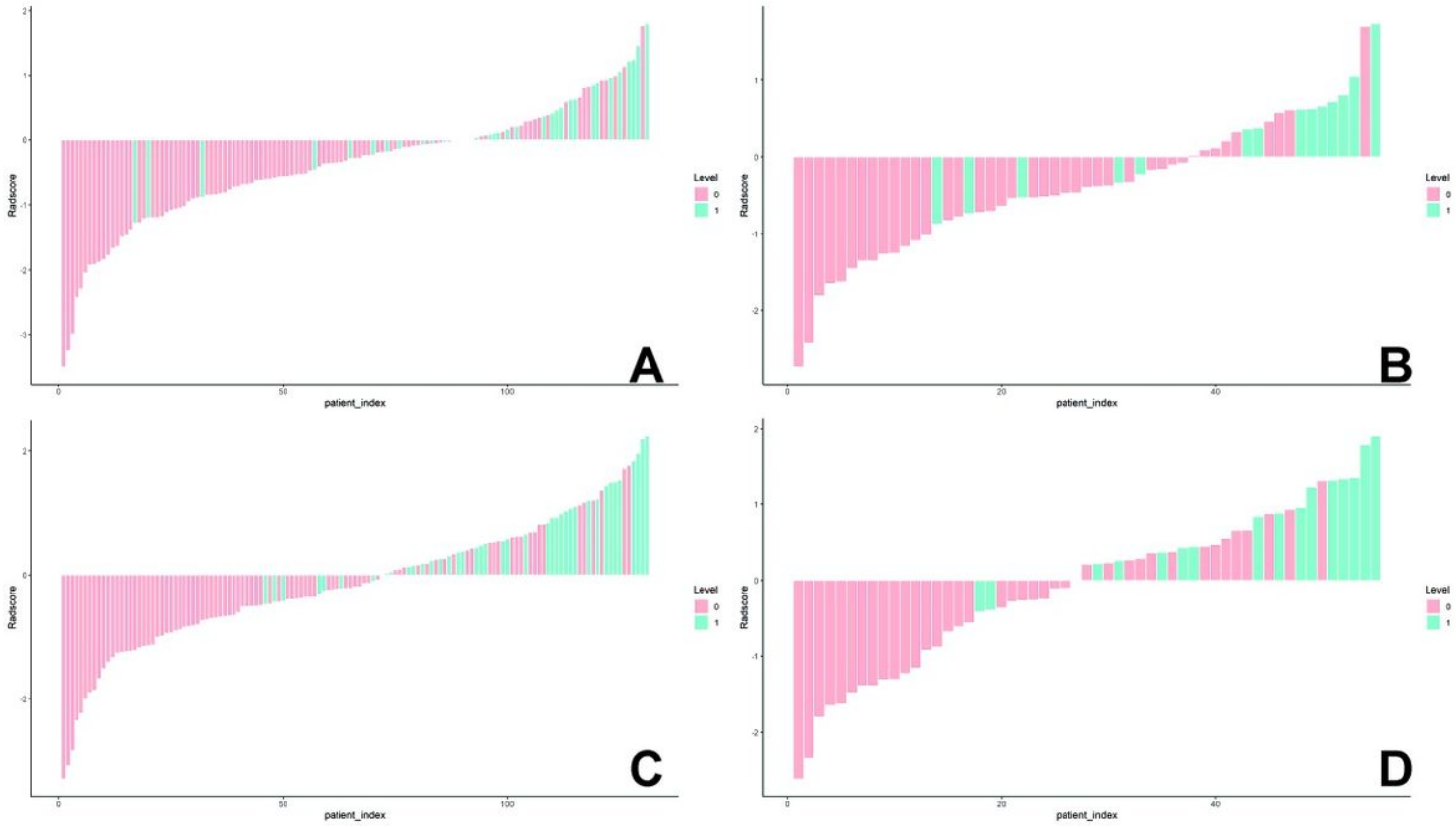

Figure 2

Radscore and radiomics nomogram-defined scores for each patient with local advanced rectal cancer (LARC). Radscore in the training cohort (A) and the validation cohort (B); radiomics nomogram-defined score in the training cohort (C) and the validation cohort (D). Red bars represent the scores for patients who did not show disease progression, while blue bars represent the scores for those who showed disease progression.

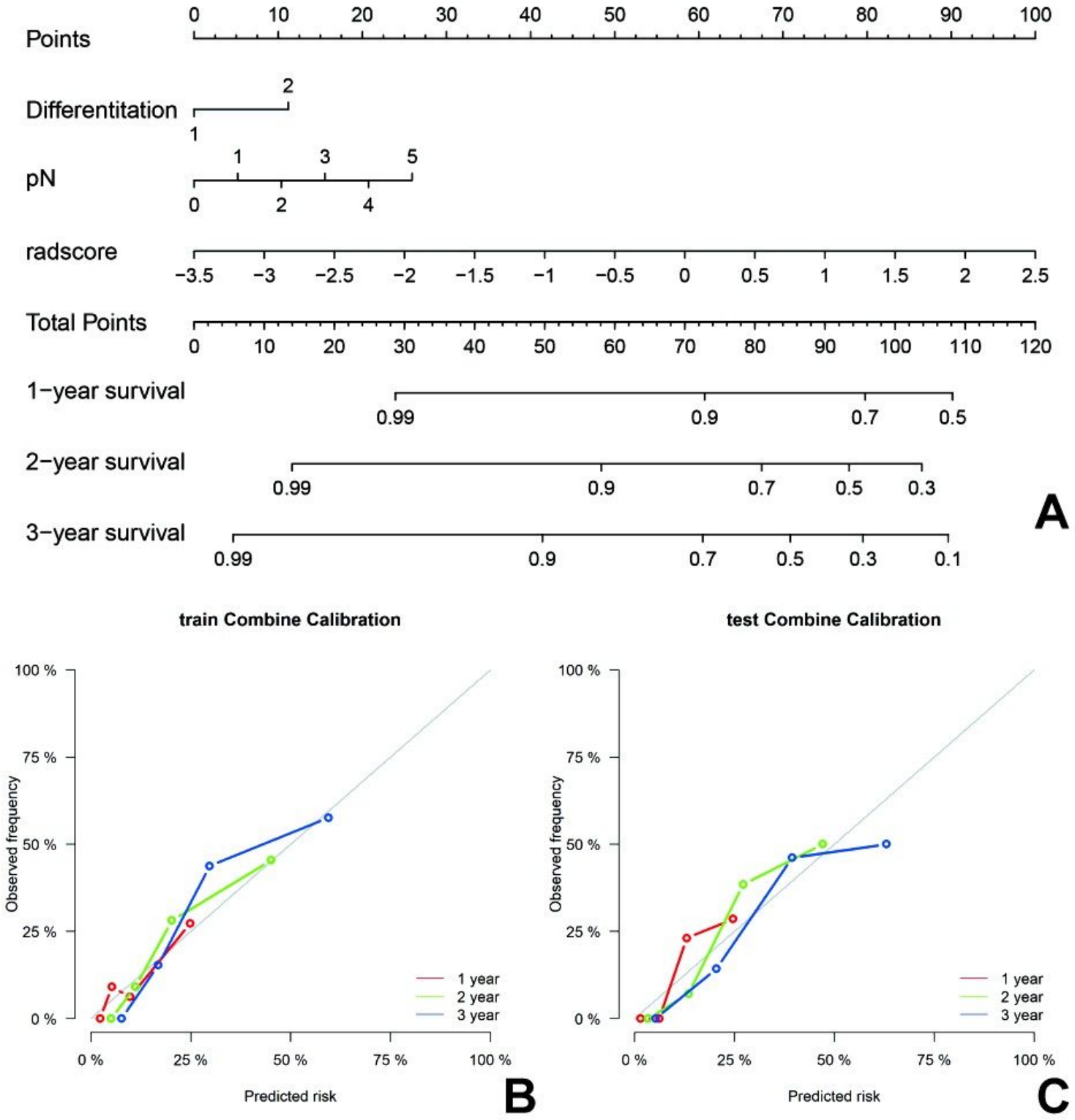

Figure 3

Nomogram for the prediction of disease-free survival (DFS) in patients with local advanced rectal cancer (LARC) (A), and the calibration curves of nomograms developed in the training (B) and validation (C) cohorts.

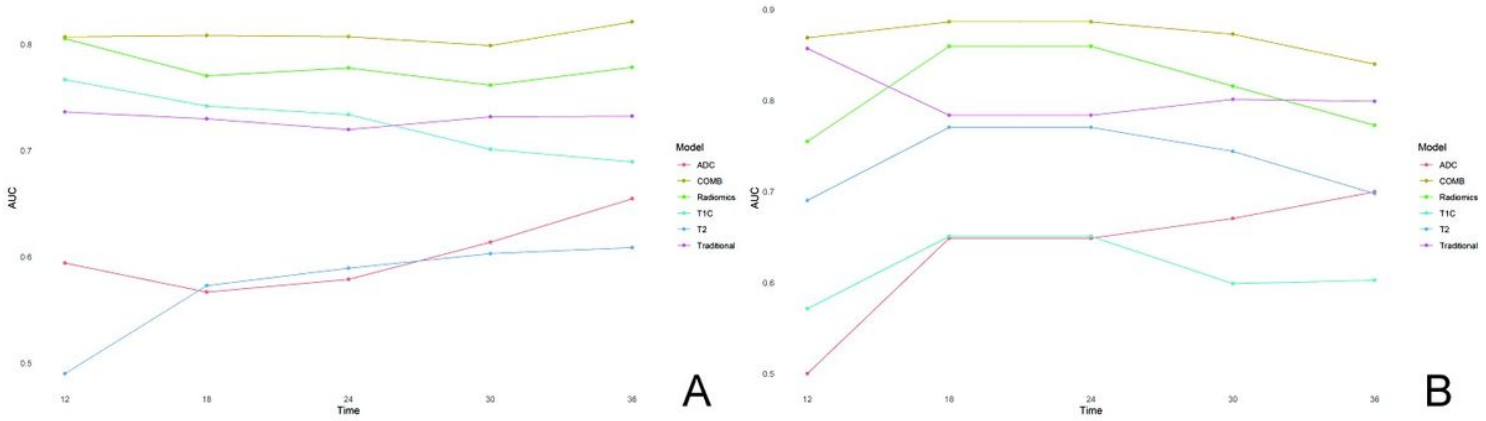

Figure 4

Discriminatory performance of all models in the training and validation cohorts. Graphs show time-dependent areas under the receiver operating characteristic (ROC) curve at various time points for different models.

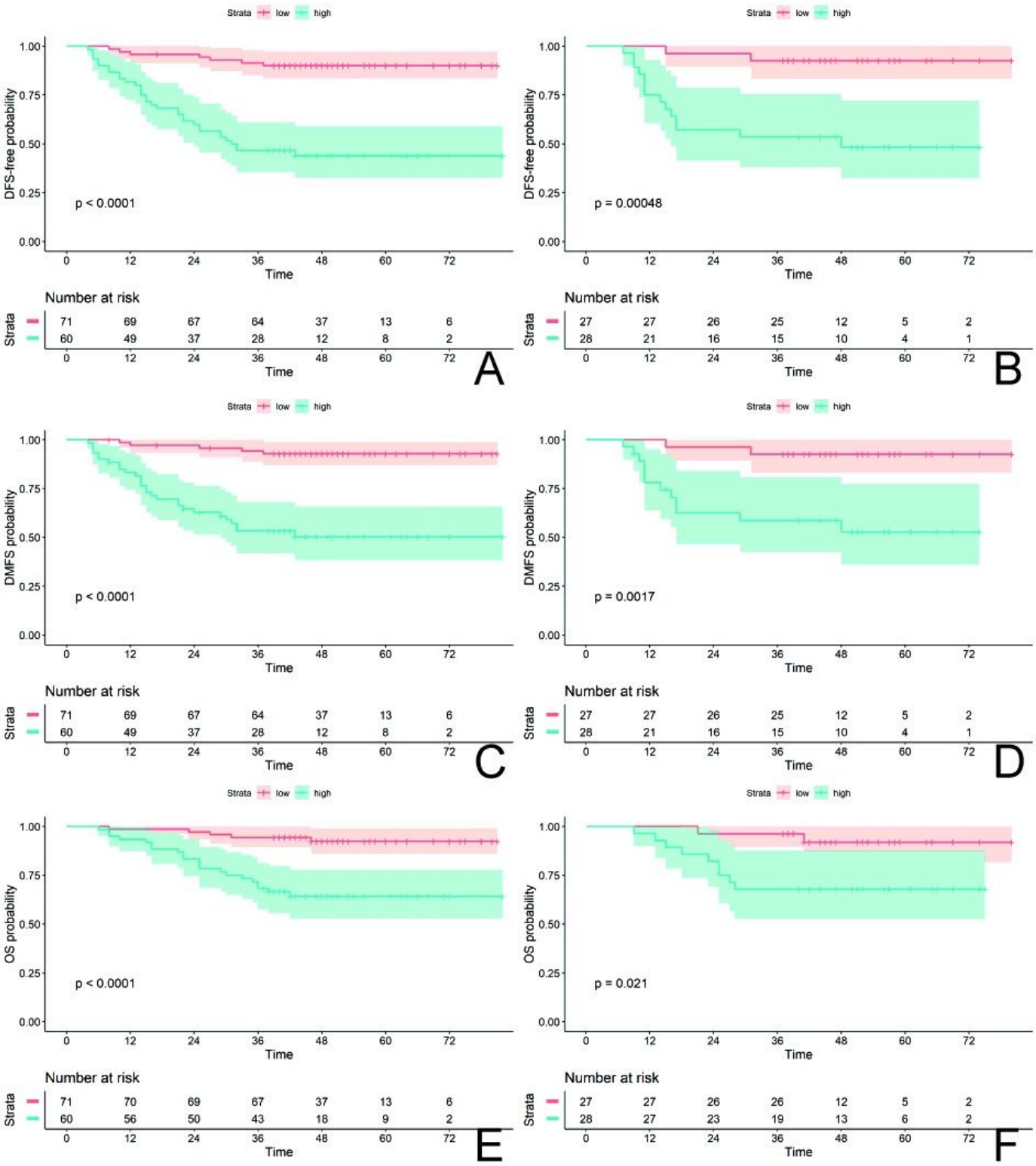

Figure 5

Disease-free survival (DFS), Distant metastasis-free survival (DMFS), and overall survival (OS) Kaplan–Meier curves between the radiomics nomogram–defined low-risk and high-risk groups in the training and validation cohorts.

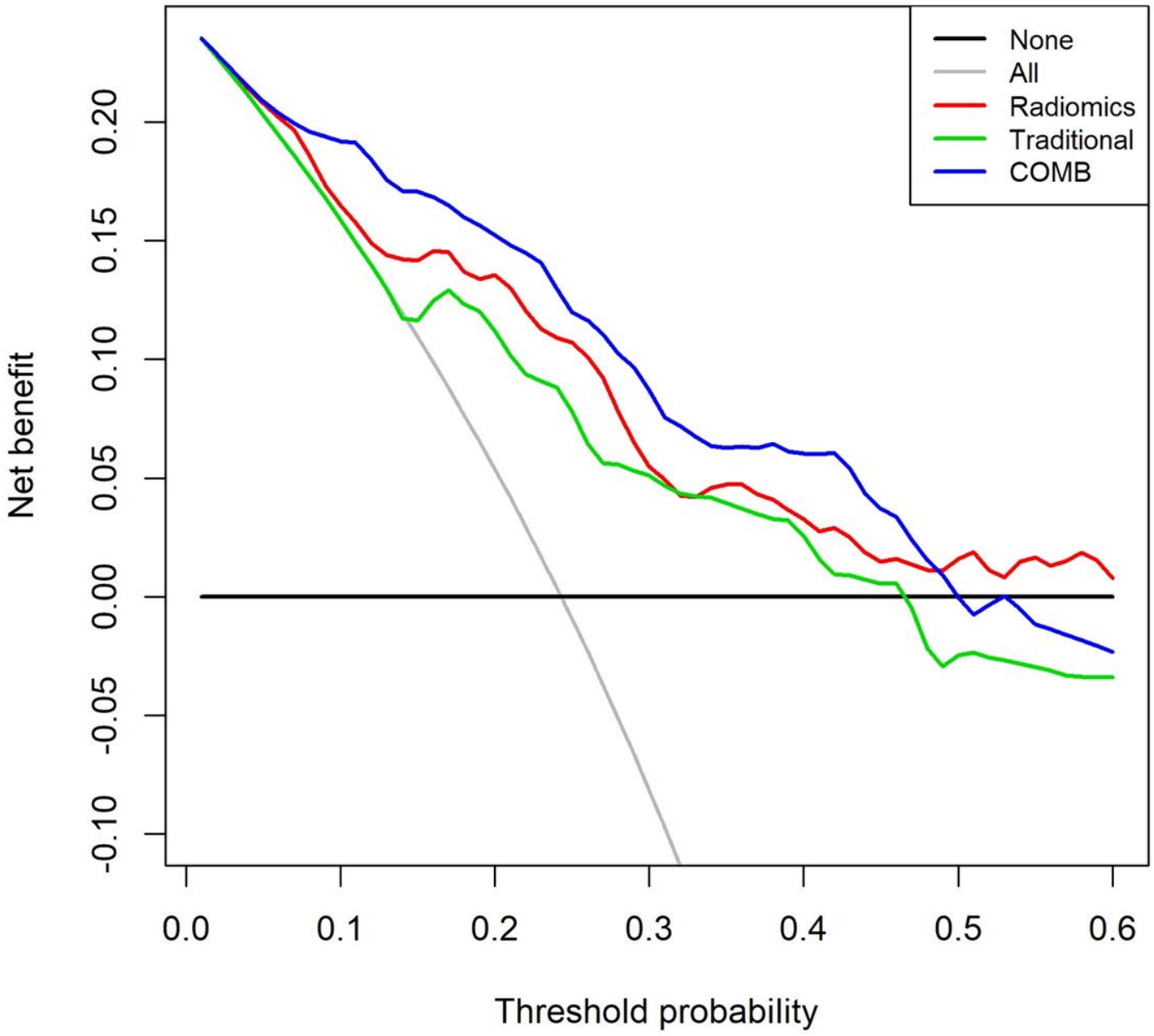

Figure 6

Decision curve analysis (DCA) for each model. The y-axis represents the net benefit. The x-axis represents the threshold probability. The radiomics nomogram added more benefit compared to both the other models and simply strategies such as follow-up of no patients (horizontal black line) or all patients (grey line) across most of the range of reasonable threshold probabilities at which a patient would choose to undergo imaging follow-up.

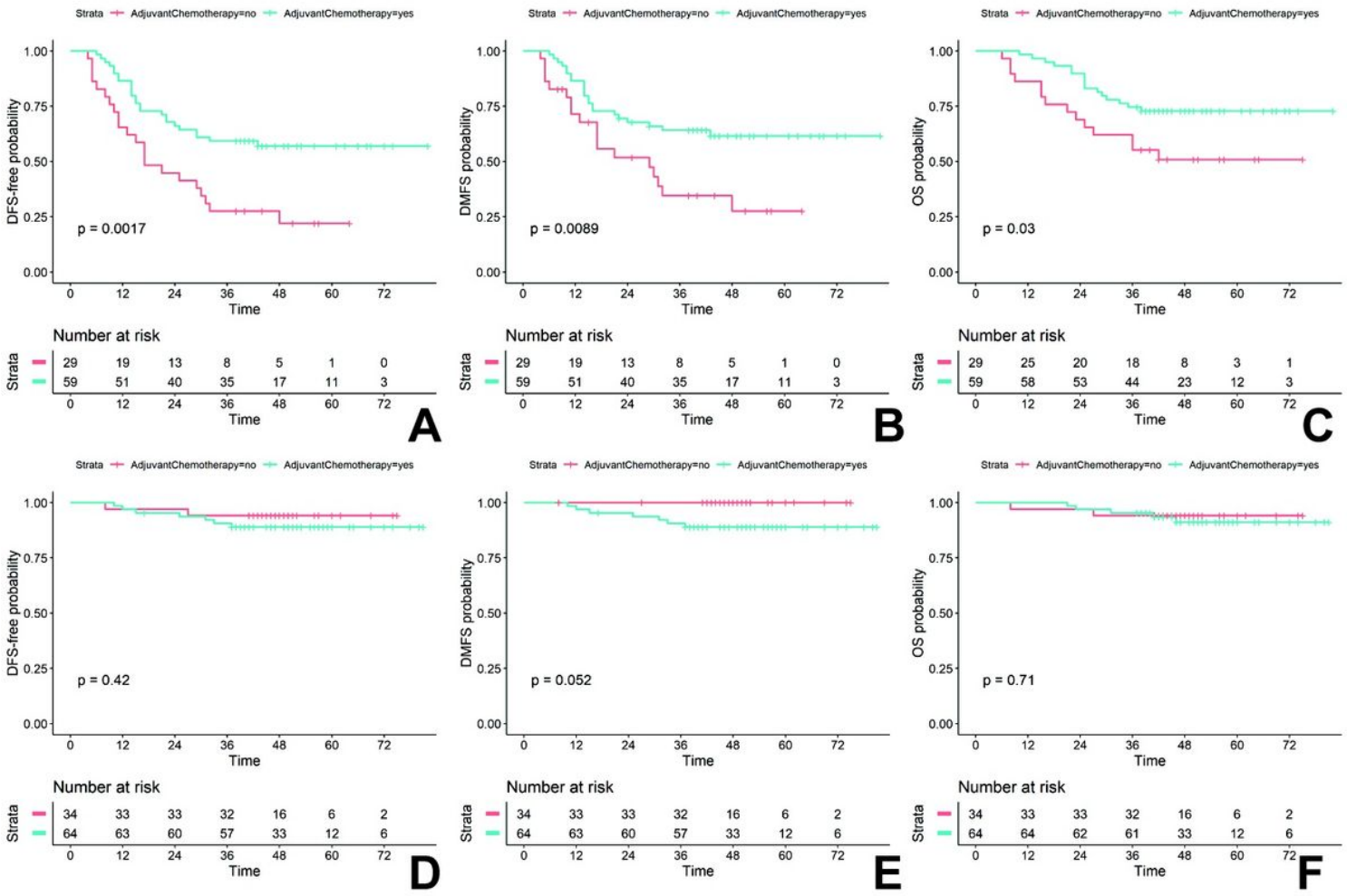

Figure 7

Disease-free survival (DFS), Distant metastasis-free survival (DMFS), and overall survival (OS) Kaplan–Meier survival curves between adjuvant chemotherapy (AC) and without AC within the radiomics nomogram–defined high-risk group (A-C) and low-risk group (D-F).

Supplementary Files

This is a list of supplementary files associated with this preprint. Click to download.

- FigureS3.tif
- FigureS3.tif
- FigureS2.tif
- FigureS2.tif
- FigureS1.tif
- FigureS1.tif
- supplemental.docx

- supplemental.docx